New Paradigm for Suppression of Gyrokinetic Turbulence by Velocity Shear

G. M. Staebler, R. E. Waltz, J. Candy, and J. E. Kinsey
General Atomics, P.O. Box 85608, San Diego, California 92186-9784, USA
(Received 28 June 2012; published 30 January 2013)

The shear in the mean field velocity Doppler shift is shown to suppress the amplitude of electric potential fluctuations by inducing a shift in the peak of the radial wave number spectrum. An analytic model of the process shows that the fluctuation spectrum shifts in the direction where the velocity shear is linearly destabilizing but that nonlinear mixing causes a recentering of the spectrum about a shifted radial wave number at reduced amplitude A model for the 2D nonlinear spectrum is used in a quasilinear calculation of the transport that is shown to accurately reproduce the suppression of energy and particle transport and the Reynolds stress due to the velocity shear.

DOI: 10.1103/PhysRevLett.110.055003 PACS numbers: 52.30.Gz, 52.35.Ra, 52.55.Fa, 52.65.Tt

The suppression of turbulence, in strongly magnetized plasmas, by shear in the mean field $E \times B$ drift velocity, due to the electric field normal to magnetic flux surfaces, was first proposed [1,2] as an explanation of the high confinement regime (H mode) observed in tokamaks [3]. The theoretical model for suppression was a temporal decorrelation of a passive scalar by advection in a field of turbulence. This paradigm was tested with nonlinear gyrofluid turbulence simulations [4]. It was found that shear in the Doppler shift due to the $E \times B$ velocity did suppress turbulence but that the strength of the suppression was an order of magnitude stronger than the decorrelation formulas [1,2] predicted. Only shear in the $E \times B$ Doppler shift or "Doppler shear" is stabilizing. A sheared velocity parallel to the magnetic field drives a Kelvin-Helmholtz type instability. It was found [4] that the ion energy flux driven by the turbulence could be modeled by a "quench rule" formula. In the quench rule paradigm the intensity of the turbulence is reduced by an overall factor of $\mathrm{Max}[(1 - \alpha_E|\gamma_{E\times B}/\gamma_{\max}|), 0]$ where $\gamma_{E\times B} = r/qd(c\partial\phi_{-1}/\partial\psi)/dr$ is the Waltz-Miller shear rate [4] of the equilibrium electric potential (ϕ_{-1}), α_E is a positive constant and $\gamma_{\max}$ is the maximum linear growth rate without Doppler shear in the simulation. This formula was shown to be robust over a range of plasma parameters. This is suggestive of an essentially linear process, even though it is a model of the nonlinear simulation results. In sheared slab geometry, a shear in the $E \times B$ velocity Doppler shift is linearly stabilizing [5] to gyrokinetic eigenmodes. However, in the axisymmetric toroidal geometry of a tokamak, the linear ballooning modes become Floquet modes, propagating along the magnetic field, when there is Doppler shear. There is no clear correspondence between the linear stability of these Floquet modes and the suppression of the turbulence [4]. The quench rule has been a successful paradigm for interpreting gyrokinetic linear stability trends in experiments [6] and for predictive quasilinear transport modeling [7].

The first indication that the quench rule was incomplete was the inability of the quasilinear models to compute the toroidal Reynolds stress driven by Doppler shear in the gyrokinetic turbulence simulations [8]. A finite Reynolds stress requires a breaking of the "poloidal parity" of the gyrokinetic equations, defined as a simultaneous reflection in poloidal angle and parallel velocity. The quench rule does not break the poloidal parity. It was first conjectured that the way in which a Reynolds stress is produced by the Doppler shear was by causing a finite spectral average radial wave number [8]. A finite radial wave number k_x was shown to break the poloidal parity of individual gyrokinetic ballooning eigenmodes and yield a finite quasilinear Reynolds stress. If the spectrum of the turbulence is symmetric with respect to the sign of the radial wave number, then the spectral average radial wave number is zero and there is no net Reynolds stress. A finite radial wave number is linearly stabilizing but this was not, by itself, enough to account for the reduction in energy transport [8]. These successes motivated a closer examination of the radial wave number spectrum of the turbulence that has lead to the new paradigm for how the Doppler shear suppresses transport reported in this Letter. Details of the verification of the new model over a range of plasma parameters, and with parallel flows, will be given in a separate paper.

The time averaged, magnetic flux-surface averaged, Fourier amplitude of the electric potential fluctuations in gyrokinetic units at a fixed poloidal $k_y = k_\theta \rho_s$ and radial $k_x = k_r \rho_s$ wave number is denoted by

$$\Phi_{k_y,k_x} = \langle |e\tilde{\phi}_{k_y,k_x}/T_e|^2 \rangle^{1/2} a/\rho_s, \tag{1}$$

where a = minor radius of plasma boundary, $\rho_s = c_s/\Omega_s$, $c_s = \sqrt{T_e/m_i}$, $\Omega_s = eB_{\mathrm{unit}}/\mathrm{cm}_i$, T_e = electron temperature, m_i = ion mass, $B_{\mathrm{unit}} = q/rd\psi/dr$, r = minor radius of poloidal magnetic flux surface ψ, and q = safety factor. All growth rates and shear rates will be in units of c_s/a. The radial wave number spectrum of the electric potential amplitude is shown in Fig. 1 (black) for nonlinear

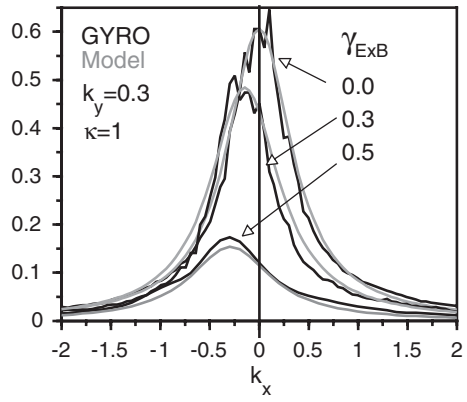

FIG. 1. Radial wave number spectrum of the time and flux surface averaged electric potential fluctuation Fourier amplitude Φ_{k_y,k_x} (black) for the GA standard case [8] with $k_y = 0.3$ and three values of the Doppler shear. Also shown are the spectral shift model spectra (gray) [Eq. (7)].

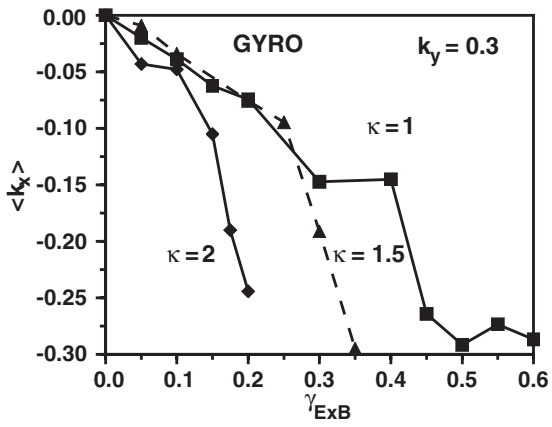

FIG. 2. The spectral average radial wave number shift [Eq. (2)] $\langle k_x \rangle$ at $k_y = 0.3$ as a function of the Doppler shear $\gamma_{E\times B}$ computed from GYRO simulations for three values of the flux surface elongation ($\kappa = 1.0, 1.5, 2.0$).

gyrokinetic turbulence simulations of the GA standard case parameters [8] with finite aspect ratio toroidal geometry and three values of the Doppler shear. The GYRO code [9] was used for the simulations in this Letter and all cases neglect magnetic fluctuations, keeping only the electric potential fluctuations. The shift of the peak of the spectrum to negative k_x and the reduction in peak amplitude, are clearly seen in Fig. 1. Note that k_x is related to the conventional ballooning angle constant [4] θ_0 by $k_x = k_y \hat{s} \theta_0$ where $\hat{s} = rdq/qdr$ is the magnetic shear and does not include the ballooning eikonal contribution to the radial wave number. A finite k_x corresponds to a tilted ballooning mode and indeed a poloidal tilt of the 2D correlation function contours is evident in the GYRO simulations with Doppler shear [8]. The model that will be presented in this Letter is also shown (gray) for these cases in Fig. 1.

In order to resolve the spectral shift, these simulations require a larger range of both poloidal and radial wave numbers than is typically needed to compute energy transport. The cases in this Letter have 32 toroidal modes up to $k_y = 1.55$ and 340 radial grid points, which can accurately resolve up to about $k_{\max} = 4.2$ (half of the maximum grid k_x) for Doppler shear ≤ 0.4 and 16 toroidal modes up to $k_y = 1.5$ with 510 radial grid points ($k_{\max} = 12.6$) for larger Doppler shear. The spectral average shift is defined by

$$\langle k_x \rangle = \int_{-\infty}^{\infty} dk_x \Phi^2_{k_y,k_x} k_x / \bar{\Phi}^2_{k_y}, \quad \text{where } \bar{\Phi}^2_{k_y} = \int_{-\infty}^{\infty} dk_x \Phi^2_{k_y,k_x}. \tag{2}$$

In Fig. 2 the spectral average shift as a function of the Waltz-Miller shear rate is shown for $k_y = 0.3$ and three different flux surface elongations ($\kappa = 1.0, 1.5, 2.0$) The GA standard case has circular flux surfaces ($\kappa = 1.0$). From Fig. 2, it is clear that the k_x shift has a nonlinear dependence on the Doppler shear rate that becomes stronger with increasing elongation. The k_x shift increases with k_y.

For the zonal flows (i.e., $k_y = 0$) the k_x spectrum is symmetric with respect to the sign of k_x and $\langle k_x \rangle$ is zero even for finite mean field Doppler shear. This is required by the reality condition on the Fourier amplitudes of the electric potential fluctuation ($\tilde{\phi}^*_{k_y,k_x} = \tilde{\phi}_{-k_y,-k_x}$). Hence, nonlinear mode coupling to the zonal flows does not contribute to the spectral shift of the finite k_y fluctuations. In these GYRO simulations, as with previous cases with kinetic electrons [10], the turbulence is not shut off (quenched) as was seen in adiabatic electron simulations [4], even for very large Doppler shear ($\gamma_{E\times B} = 0.8$).

Over the resolved k_x range, the spectral shape without Doppler shear is very well fit by the Lorentzian function

$$\Phi_{\text{model}} = \frac{\gamma^{\text{eff}}_{k_y}}{(c_y k_y^2 + c_x k_x^2)}, \quad \text{where } \gamma^{\text{eff}}_{k_y} = c_y k_y^2 \Phi_{k_y,k_x}|_{k_x=0}. \tag{3}$$

The coefficient c_y is arbitrary, $\gamma^{\text{eff}}_{k_y}$ is an effective nonlinear growth rate, and $c_x = 0.56 c_y$ is chosen to make the integrated intensity match ($\bar{\Phi}^2_{k_y} = \bar{\Phi}^2_{\text{model}}$) at $k_y = 0.3$. For $k_y > 0.05$ this model [Eq. (3)] fits the shape of the GYRO spectrum with an average standard deviation of 12% with the same value of c_x/c_y.

The shift in the k_x-spectrum induced by the Doppler shear can be qualitatively modeled with an analytic nonlinear Bernoulli differential equation.

$$\frac{d\Phi_{\text{model}}}{dt} = \gamma^{\text{eff}}_{k_y} \Phi_{\text{model}} + \gamma_{E\times B} k_y \frac{\partial \Phi_{\text{model}}}{\partial k_x} - (c_y k_y^2 + c_x k_x^2) \Phi^2_{\text{model}} = 0. \tag{4}$$

This is an interpretive model of the nonlinear saturation of the amplitude of the electric potential fluctuations. The first two terms are the linear growth $\gamma_{k_y}^{\rm eff}$ and the Fourier transform of the radial variation of the $E \times B$ velocity Doppler shift about a flux surface r_s: $ik_y\gamma_{E\times B}(r - r_s)/\rho_s \rightarrow k_y\gamma_{E\times B}\partial/\partial k_x$ that can be derived directly from the linear gyrokinetic equation. The third quadratic nonlinear term represents the effect of the fluctuating $E \times B$ nonlinear mode coupling. The actual nonlinear mode coupling term in the gyrokinetic equation [11] is a convolution over the 2D wave number space (k_x, k_y). The model nonlinear term in Eq. (4) is local in (k_x, k_y) but it has the same wave number and field powers as the physical nonlinearity and it gives the correct GYRO spectrum [Eq. (3)] for zero Doppler shear. Without the nonlinear term, and identifying $\gamma_{k_y}^{\rm eff} \rightarrow \frac{\partial}{\partial t}$, Eq. (4) has traveling wave solutions $\Phi_{\rm model} = \Phi_{\rm model}(k_x - k_y\gamma_{E\times B}t)$ related to the Floquet modes [4]. The nonlinear term localizes the traveling waves to a standing wave form $\Phi_{\rm model} = \Phi_{\rm model}(k_x + k_y\gamma_{E\times B}/\gamma_{k_y}^{\rm eff})$. The model equation Eq. (4) can be solved analytically. Substituting $\Phi_{\rm model} = {\rm Exp}[-(k_x\gamma_{k_y}^{\rm eff})/(k_y\gamma_{E\times B})]/K$ into Eq. (4) gives a linear equation for the function $K(k_x)$.

$$k_y\gamma_{E\times B}\frac{\partial K}{\partial k_x} = -{\rm Exp}\left[-\frac{k_x\gamma_{k_y}^{\rm eff}}{k_y\gamma_{E\times B}}\right](c_yk_y^2 + c_xk_x^2) \qquad (5)$$

Integrating Eq. (5) shows how the tilt, from the odd in k_x exponential factor due to the $E \times B$ shear, becomes averaged, by the symmetric shape of the spectrum, into a new spectrum symmetric about a shifted peak. Choosing the integration constant so that the solution reduces to Eq. (3) for $\gamma_{E\times B} \rightarrow 0$ gives

$$\Phi_{\rm model} = \gamma_{k_y}^{\rm eff}/[c_yk_y^2 + c_x\langle k_x\rangle_{\rm model}^2 + c_x(k_x - \langle k_x\rangle_{\rm model})^2], \qquad (6)$$

where $\langle k_x\rangle_{\rm model} = -k_y\gamma_{E\times B}/\gamma_{k_y}^{\rm eff}$. The notation anticipates the result that $\langle k_x\rangle_{\rm model}$ is the spectral average shift [Eq. (2)] evaluated using the model amplitude [Eq. (6)]. The model solution [Eq. (6)] captures the primary qualitative features of the GYRO spectrum [Fig. 1] that the peak shifts and the amplitude is reduced. The direction of the shift is governed by the sign of the Doppler shear. The unshifted spectrum [Eq. (3)] substituted into Eq. (4) yields a Doppler shear term that is linearly destabilizing for $k_y\gamma_{E\times B}\partial\Phi_{\rm model}/\partial k_x > 0$. The interaction with the nonlinear term recenters the spectrum about a new peak in the destabilized direction. The numerator of the solution $(\gamma_{k_y}^{\rm eff})$ is unchanged by the shift. The Lorentzian shape of the model spectrum about the peak is also unchanged by the shift but the peak amplitude is reduced by the factor $(1 + c_x\langle k_x\rangle_{\rm model}^2/c_yk_y^2)^{-1}$. The suppression of the turbulence is due to the nonlinear recentering response to the Doppler shear induced linear destabilization that preserves the Lorentzian shape about the peak.

The model solution Eq. (6) does not match the GYRO spectrum in two important details. The linear relation between the spectral average shift and the Doppler shear has the right sign, but it cannot fit the GYRO results in Fig. 2. So the actual shift is used in the final model. The shifted peak amplitude in the GYRO spectrum [Fig. 1] is below the curve of the unshifted spectrum, whereas the model spectrum peak is on the unshifted curve. This defect of the model equation solutions is true even if the linear growth rate as a function of k_x is used in the nonlinear Bernoulli equation [Eq. (4)] instead of $\gamma_{k_y}^{\rm eff}$. Clearly, the decay of the linear growth rate with k_x/k_y plays some role in determining the shape of the GYRO spectrum, but the simplified nonlinearity in the model equation does not reproduce that physics. In order to fit the reduction of the peak of the GYRO spectrum, a reduction factor that depends only on the spectral average shift is applied to the model spectrum [Eq. (6)].

$$\Phi_{ss} = \frac{\gamma_{k_y}^{\rm eff}/[1 + (\alpha_x\langle k_x\rangle/k_y)^4]}{[c_yk_y^2 + c_x\langle k_x\rangle^2 + c_x(k_x - \langle k_x\rangle)^2]}. \qquad (7)$$

This is the final model that was used to fit to the GYRO spectra in Fig. 1. It has the feature that it depends only on the spectral shift $\langle k_x\rangle$ computed from the GYRO spectra and not directly on the Doppler shear. Hence, it will be called the "spectral shift" model. The fit of the spectral shift model [Eq. (7)] to the GYRO spectrum is illustrated in Fig. 1 by the gray lines. The fitting coefficient in the amplitude reduction factor in Eq. (7) was determined to be $\alpha_x = 1.15$. In Fig. 3, the integrated intensity $\bar{\Phi}_{ss}^2$ for the spectral shift model [Eq. (7)] is compared to the GYRO results as a function of the Doppler shear for three different flux surface elongations. Using the GYRO simulation values of the spectral shift in the model [Eq. (7)] produces a good

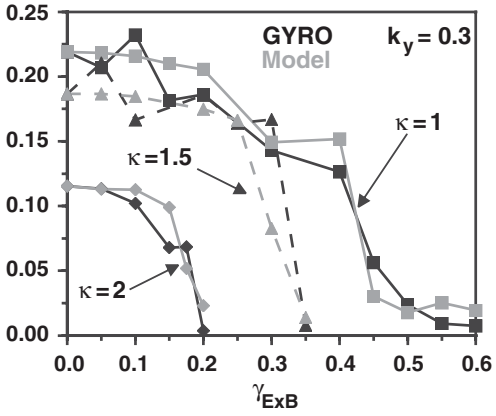

FIG. 3. Integrated intensity $\bar{\Phi}_{k_y}^2$ [Eq. (2)] at $k_y = 0.3$ as a function of Doppler shear $\gamma_{E\times B}$ for three values of the flux surface elongation ($\kappa = 1.0$, 1.5, 2.0) comparing the GYRO results (black) with the spectral shift model (gray) [Eq. (7)].

fit to the intensity, for all three elongations, for the same values of the fit parameters $(c_x/c_y, \alpha_x)$. This demonstrates that the suppression of the turbulence has a simpler relationship to the spectral shift than it does to the Doppler shear. The verification of the spectral shift model [Eq. (7)] for a large number of GYRO parameter scans will be presented in a future paper. The two fitting coefficients $(c_x/c_y, \alpha_x) = (0.56, 1.15)$ in Eq. (7) have been found to depend only weakly on plasma parameters (safety factor, magnetic shear, trapped fraction, elongation, Ti/Te). The spectral width is increased by the shift $\langle k_x^2 \rangle = (c_y k_y^2/c_x) \times (1 + 2c_x \langle k_x \rangle^2/(c_y k_y^2))$. This is similar to the formula for the change in the inverse radial correlation length squared from the decorrelation model [12] that is quadratic in the $E \times B$ velocity shear. However, the decorrelation rate reduction that results from the peak amplitude reduction of Eq. (7) is much stronger than the decorrelation formulas [1,2].

A direct consequence of the shift in the k_x-spectrum is the breaking of poloidal parity, which results in a finite Reynolds stress [8]. In order to illustrate this, the transport will be computed quasilinearly, using the spectral shift model [Eq. (7)] for the electric potential and a linear eigenmode calculation of the quasilinear weights. The Trapped Gyro-Landau Fluid (TGLF) equations [13] are a reduced 15-moment fluid model for the linear gyrokinetic equation. They have been verified to be an accurate model for computing the linear eigenmodes. The values of the unshifted peak of the electric potential spectrum, and the spectral shift $\langle k_x \rangle$ from the GYRO simulation, are used in the spectral shift model [Eq. (7)]. The TGLF model is used to compute the linear eigenmodes of the most unstable drift-ballooning mode at the (k_y, k_x) values of the shifted peak. The quasilinear formulas for the electron particle flux, the electron energy flux, the ion energy flux and the toroidal ion Reynolds stress are, respectively,

$$\begin{aligned}
\Gamma_e &= c_0 \sum_{k_y} \Delta k_y \Phi_{ss}^2 \{\tilde{v}_{E\times B} \tilde{n}_e / \tilde{\phi}^2\}|_{k_y, \langle k_x \rangle}, \\
Q_e &= c_0 \frac{3}{2} \sum_{k_y} \Delta k_y \Phi_{ss}^2 \{\tilde{v}_{E\times B} \tilde{p}_e / \tilde{\phi}^2\}|_{k_y, \langle k_x \rangle}, \\
Q_i &= c_0 \frac{3}{2} \sum_{k_y} \Delta k_y \Phi_{ss}^2 \{\tilde{v}_{E\times B} \tilde{p}_i / \tilde{\phi}^2\}|_{k_y, \langle k_x \rangle}, \\
\Pi_{i,\mathrm{tor}} &= c_0 R_0 \sum_{k_y} \Delta k_y \Phi_{ss}^2 \{\tilde{v}_{E\times B} \tilde{v}_{i,\mathrm{tor}} / \tilde{\phi}^2\}|_{k_y, \langle k_x \rangle}.
\end{aligned} \tag{8}$$

The curly brackets contain the quasilinear weights evaluated using the TGLF linear eigenfunction moments. All of these are in gyrokinetic units [13]. The results for the GA standard case are shown in Fig. 4. The overall factor c_0 was chosen to fit the ion energy flux [Fig. 4(b)] at zero Doppler shear. The quasilinear weights determine the ratios of the fluxes quite well. The reduction of all of the fluxes with the Waltz-Miller shear is fit very well by the quasilinear model. The Reynolds stress [Fig. 4(a)] is due to the parity breaking of the linear eigenmodes by the finite k_x. The good agreement between the quasilinear model and the nonlinear GYRO results shows that the ballooning eigenmode at the peak of the shifted spectrum is the most important linear mode in the nonlinear spectrum.

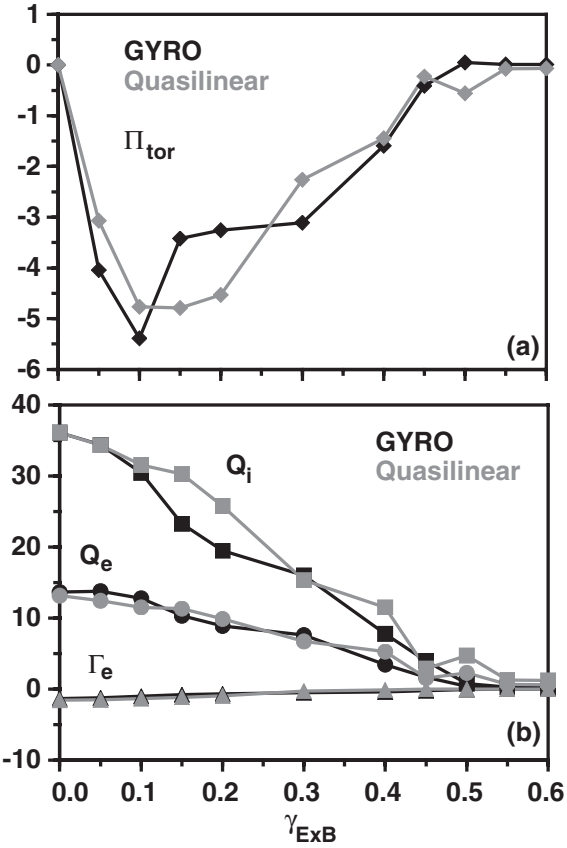

FIG. 4. Toroidal Reynolds stress (a) and electron and ion energy flux and particle flux (b) from GYRO simulations (black) and the spectral shift quasilinear model [Eq. (8)] (gray) as a function of Doppler shear rate for the GA standard case [8].

Neither the quench rule nor the decorrelation model can produce a Reynolds stress from the Doppler shear since they only reduce the intensity. It is remarkable that fitting the properties of the k_x spectrum for the electric potential, from the nonlinear GYRO simulations, results in such an accurate quasilinear model of the suppression of transport and the generation of a Reynolds stress by Doppler shear.

In this Letter, a new paradigm for the way in which $E \times B$ velocity shear suppresses gyro-kinetic turbulence has been presented. The shear in the $E \times B$ velocity Doppler shift produces a shift in the peak, and a reduction in amplitude, of the radial wave number spectrum of electric potential fluctuations. These features are qualitatively reproduced by an analytic model of the nonlinear saturation. The model shows that the spectrum shift is caused by the Doppler shear being linearly destabilizing on one side and stabilizing in the opposite side of the peak. The nonlinear mixing recenters and resymmetrizes the

spectrum about a peak in the destabilizing direction, which reduces the amplitude of the peak. The net suppression depends only on the spectral shift $\langle k_x \rangle$. This is a very different paradigm than the decorrelation [1,2] and quench rule [4] paradigms. The new spectral shift paradigm also captures the finite-k_x tilted ballooning eigenmode parity breaking that generates a finite Reynolds stress from the Doppler shear. The Reynolds stress due to the Doppler shear is a momentum pinch that can contribute to a finite toroidal rotation even when there is no external torque [8]. The spectral shift paradigm provides a framework to understand how more general radial variations of the equilibrium profiles, present in global gyrokinetic simulations [14,15], can generate a Reynolds stress and suppress transport.

This work was supported in part by the US Department of Energy under No. DEFG0295ER54309 and No. DEFC0204ER 54698.

[1] K. C. Shaing, E. C. Crume, and W. A. Houlberg, Phys. Fluids B **2**, 1492 (1990).
[2] H. Biglari, Phys. Fluids B **2**, 1 (1990).
[3] F. Wagner *et al.*, Phys. Rev. Lett. **49**, 1408 (1982).
[4] R. E. Waltz, R. L. Dewar, and X. Garbet, Phys. Plasmas **5**, 1784 (1998).
[5] G. M. Staebler and R. R. Dominguez, Nucl. Fusion **31**, 1891 (1991).
[6] K. H. Burrell, Plasma Phys. Controlled Fusion **36**, A291 (1994), and references cited therein.
[7] J. E. Kinsey, G. M. Staebler, and R. E. Waltz, Phys. Plasmas **12**, 052503 (2005).
[8] G. M. Staebler, R. E. Waltz, and J. E. Kinsey, Phys. Plasmas **18**, 056106 (2011).
[9] J. Candy and R. E. Waltz, J. Comput. Phys. **186**, 545 (2003).
[10] J. E. Kinsey, R. E. Waltz, and J. Candy, Phys. Plasmas **12**, 062302 (2005).
[11] E. A. Frieman and Lui Chen, Phys. Fluids **25**, 502 (1982).
[12] T. S. Hahm and K. H. Burrell, Phys. Plasmas **2**, 1648 (1995).
[13] G. M. Staebler, J. E. Kinsey, and R. E. Waltz, Phys. Plasmas **12**, 102508 (2005).
[14] R. E. Waltz, G. M. Staebler, and W. M. Solomon, Phys. Plasmas **18**, 042504 (2011).
[15] Y. Camenen, Y. Idomura, S. Jolliet, and A.G. Peeters, Nucl. Fusion **51**, 073039 (2011).